

## Phase Determination by Polarized Dispersion in Vanadyl Sulfate Pentahydrate

BY DAVID H. TEMPLETON AND LIESELOTTE K. TEMPLETON

*Department of Chemistry, University of California, Berkeley, CA 94720, USA*

(Received 2 November 1990; accepted 13 February 1991)

### Abstract

Anomalous-scattering tensors for V measured with linearly polarized synchrotron radiation in  $\text{VOSO}_4 \cdot 5\text{H}_2\text{O}$  near the  $K$ -absorption edge exhibit anisotropy as much as 4 units in  $f''$  and  $\pm 2$  units in  $f'$ . This polarized dispersion causes the diffraction intensity to change when a crystal is turned around a diffraction vector and is the basis of a new way to obtain phases of structure factors.

### 1. Introduction

The method of isomorphous replacement (Cork, 1927) has long been used to solve the structure-factor phase problem in Fourier analysis of crystal structures. Its essence is to change the scattering factor at a site or sites in the unit cell by substitution of atoms. Sometimes such substitution is difficult to achieve and other methods are needed. A similar method is based on the dispersion of atomic scattering as the wavelength changes. This multiwavelength anomalous-dispersion (MAD) method also has a long history (Okaya & Pepinsky, 1956; Ramaseshan, Venkateshan & Mani, 1957) but was used infrequently until synchrotron radiation provided the wavelengths needed for best results (e.g. Guss, Merritt, Phizackerley, Hedman, Murata, Hodgson & Freeman, 1988; Hendrickson, Pähler, Smith, Satow, Merritt & Phizackerley, 1989). Another way to determine phases by modulation of the scattering at specific atomic sites was suggested by Templeton & Templeton (1985a) and here we demonstrate its use. This 'polarized dispersion method' depends on a change of atomic scattering factor for polarized X-rays as the crystal is turned in azimuth with the  $\mathbf{h}$  vector as axis.

The amplitude and phase of scattering of X-rays by atoms change abruptly with wavelength at the absorption edges, the photon energies just sufficient to excite specific inner electrons. For a long time the anomalous-scattering terms  $f'$  and  $f''$  which describe the real and imaginary parts of this dispersion of the complex scattering factor were assumed to be scalar properties independent of photon polarization. This assumption is invalid when the electrons are excited to states whose symmetries reflect anisotropic chemical structure and bonding. Then one needs anisotropic tensors to describe the variation of these

properties with polarization directions of incident and scattered beams (Templeton & Templeton, 1982; Dmitrienko, 1983).

Fanchon & Hendrickson (1990) described in detail how one can take account of polarized dispersion in applications of the MAD method. While their main objective was to avoid errors caused by this birefringence, they mentioned that it could be used to determine phases with a single wavelength. Their exposition allows us to simplify our discussion here.

The vanadyl ion  $\text{VO}^{2+}$  has a polarized pre-edge absorption line near the  $K$  edge (Templeton & Templeton, 1980). First we report measurements of the vanadium scattering tensor near this line by absorption spectroscopy and diffraction techniques using linearly polarized X-rays at the Stanford Synchrotron Radiation Laboratory. Then we describe how this polarized dispersion can be used to solve the structure-factor phase problem.

Tachez, Théobald, Watson & Mercier (1979) refined the crystal structure of vanadyl sulfate pentahydrate with data measured using Mo  $K\alpha$  radiation. Crystal data are: monoclinic,  $P2_1/c$ ,  $a = 6.976$  (2),  $b = 9.716$  (5),  $c = 12.902$  (4) Å,  $\beta = 110.90$  (3)°,  $Z = 4$ . In this structure the directions of the V–O bonds of the vanadyl ions are 82.6 or 97.4° from  $\mathbf{b}$  and their projections on the  $xz$  plane are within 0.3° of  $\mathbf{c}^*$ . A consequence is that the anisotropy of the macroscopic X-ray tensor is nearly the same as that of the atomic tensor and two of its principal axes are close to  $\mathbf{a}$  and  $\mathbf{c}^*$ . The third coincides with  $\mathbf{b}$  by symmetry.

### 2. Experimental

Monoclinic crystals of  $\text{VOSO}_4 \cdot 5\text{H}_2\text{O}$  were found in reagent 'vanadium sulfate' (Fairmount Chemical Co.). They gain or lose water in air of variable humidity, but are stable if glued to glass fibers and then dipped in fingernail polish which dries to form a thin protective coating. Enclosure in glass was avoided to simplify correction for absorption at the wavelengths near 2.27 Å. An Enraf-Nonius CAD-4 diffractometer on Beam Line 1-5 at SSRL (Phillips, Cerino & Hodgson, 1979) was used in the ways described by Templeton & Templeton (1985a, 1988b) to measure absorption spectra and diffraction intensities. The fluorescence technique was used to measure the

absorption as a function of polarization direction for a rather angular crystal, about  $0.21 \times 0.24 \times 0.36$  mm in size. The energy resolution was about 0.3 eV with a pair of Si (220) crystals in the monochromator. The horizontal polarization direction was set parallel to the reciprocal vectors 0, 0, 1 and 2, 0, -1 for the two spectra used to derive principal values of  $f''$  and  $f'$ .

An Si (111) monochromator ( $\Delta E$  ca 0.5 eV) was used for diffraction experiments. A vanadyl sulfate pentahydrate crystal, about  $0.36 \times 0.41 \times 0.48$  mm with rounded edges, was described by 19 faces for calculation of isotropic absorption by analytical integration. A further correction for the anisotropic absorption (dichroism) is described below. The energy scale was calibrated using 5463.9 eV (Bearden, 1967) for the first inflection at the *K* edge measured by transmission with a metallic vanadium foil. The working standard during experiments was the peak of the pre-edge line of polycrystalline vanadyl sulfate; we measured it to be 5468.9 (2) eV on this scale. In our spectra its width (FWHM) was 2.2 eV, about twice the minimum set by our energy resolution and the 1.0 eV natural width of the *K* level (Krause & Oliver, 1979). The ratio of horizontal to vertical linear polarization of the beam was 31.1 (6) (93.8% polarization) according to a test with a germanium Borrmann-effect filter (Cole, Chambers & Wood, 1971; Templeton & Templeton, 1988a).

Integrated intensities were measured at various azimuthal angles and several wavelengths in the vicinity of the absorption line. One procedure was to measure each of many reflections at  $\psi = -40, 0$  and  $40^\circ$ . Another was to measure a few at many  $\psi$  settings. Data were adjusted for beam variation according to readings of an ion chamber filled with helium. In some sets there was a second adjustment according to repeated measurements of a standard reflection.

### 3. Calculation of scattering factors

To derive atomic scattering factors from our diffraction data we need the parameters which describe the structure and its thermal motion. Tachez *et al.* (1979) did not include dispersion terms in their least-squares calculations. To avoid a bias from this omission, we recovered the structure factors from their Supplementary Material and repeated the refinement using  $f'$  and  $f''$  for V, S and O from Cromer & Liberman (1970). The most significant change in parameters for our purposes was an increase of  $0.08 \text{ \AA}^2$  in each  $B_{ii}$  of vanadium. The *B* values for hydrogen decreased  $0.8 \text{ \AA}^2$  on the average and their positions shifted by as much as  $0.1 \text{ \AA}$ . Other changes were about one standard deviation or less and  $R = 0.022$  was the same.

Dichroism modified the absorption factor in some of the experiments by as much as  $\pm 22\%$  during an azimuthal rotation and this variation tended to

obscure the changes due to the birefringence of the scattering factor. We have not invented a practical way to make a rigorous correction for the combinations of polarization components with their various absorption parameters. However, since the incident radiation was highly polarized and most of the intensity was in the *ss* combination of scattering (the only one with a single absorption parameter), an approximate correction can be made if the other components are neglected. We assume that the absorption tensor of each vanadium atom is uniaxial with its axis parallel to the V–O bond direction. The macroscopic absorption parameter can be written as

$$\mu = \mu_a(1 + K \mathbf{s}^T \mathbf{M} \mathbf{s}), \quad (1)$$

where  $\mathbf{s}$  is the unit polarization vector, *T* indicates transpose and  $\mu_a$  is the average of an atomic tensor for all directions of polarization (*cf.* Appendix). For this crystal structure the matrix **M** is

$$\mathbf{M} = \begin{pmatrix} -0.3333 & 0 & 0.0054 \\ 0 & -0.3167 & 0 \\ 0.0054 & 0 & 0.6500 \end{pmatrix} \quad (2)$$

in a Cartesian system with axes parallel respectively with **a**, **b** and **c\***. The factor *K* varies with wavelength according to the sign and magnitude of the anisotropy and was adjusted by trial and error during the least-squares calculations. Rather than making repeated iterations of the laborious absorption correction with individual parameters for each reflection at each azimuth, we multiplied each intensity by a second absorption factor proportional to  $\mu$  from (1). This is a good approximation for a highly absorbing crystal like this one.

A scale factor and the six independent elements of the  $f'$  tensor for vanadium were adjusted by the method of least squares, holding constant the atomic coordinates and thermal parameters. This method uses the combined scattering power of sulfur, oxygen and hydrogen as the basis for the absolute scale. In another calculation the independent variables were the scale factor and the principal values of  $f'$ :  $f'_o$  for parallel and  $f'_n$  for perpendicular polarization. The axis of the tensor was constrained to the direction of the V–O bond. No attempt was made to derive values of  $f''$  from these diffraction data because it has little effect on the intensity of scattering by this centrosymmetric crystal. The structure-factor calculations included *ss* and *sp'* terms but *pp'* and *ps* were neglected. The  $f''$  contributions were included but their polarization anisotropy was neglected.

The results listed in Table 1 were obtained using atomic parameters from our refinement of the data of Tachez *et al.* (1979). When their parameters were used, each  $f'$  was more negative by about 0.08 units. The data measured at 5472.4 eV were too few for valid determination of six components of the tensor.

Table 1. Tensor components for  $f'$  of vanadium

E(eV)	5462.5	5467.7	5470.5	5472.4
$f'_{11}$	-6.71 (12)	-6.7 (4)	-7.5 (3)	-
$f'_{22}$	-6.69 (13)	-7.5 (2)	-7.8 (1)	-
$f'_{33}$	-7.12 (9)	-9.1 (1)	-5.8 (1)	-
$f'_{12}$	-0.04 (9)	0.0 (2)	0.0 (1)	-
$f'_{13}$	0.03 (7)	-0.1 (2)	-0.1 (1)	-
$f'_{23}$	0.06 (9)	0.4 (2)	-0.2 (1)	-
$f''_{\pi}$	-6.71 (7)	-7.24 (15)	-7.71 (10)	-8.8 (4)
$f''_{\sigma}$	-7.11 (8)	-9.07 (12)	-5.72 (9)	-7.0 (2)
$\delta'$	-0.4 (1)	-1.8 (2)	2.0 (1)	1.8 (5)
R	0.052	0.069	0.057	0.042
$n^*$	324	233	257	56

\* Number of observations.

The other three data sets yielded tensor components that are consistent, within the estimated errors, with uniaxial symmetry aligned with the V-O bond. In each case the two-component refinement gives a more precise estimate of the principal values.

The fluorescence spectra were multiplied by  $1/\lambda$ , then scaled and offset to connect with  $f''$  values from the *FPRIME* program (Cromer, 1983) at a distance on either side of the edge. The resulting  $f''$  data were transformed to  $f'$  by Kramers-Kronig inversion using a difference method (Templeton & Templeton, 1988b). A correction was made for the fact that the polarization directions in the experiments did not quite coincide with the atomic tensor axes by taking linear combinations of these curves. The resulting principal values of  $f'$  and  $f''$  are shown as curves in Fig. 1. The differences from the uncorrected curves are almost invisible at this scale. Principal values of  $f'$  from the diffraction experiments are shown as points; their error bars indicate standard deviations. Curves of  $f' + if''$  in the complex plane (Fig. 2) show an extra loop for the  $\sigma$  values near the absorption line that is similar in size to that at the edge.

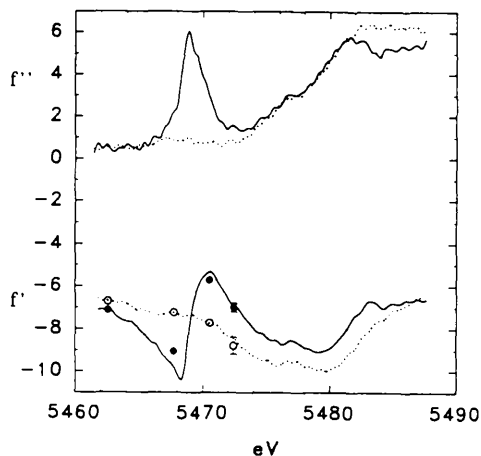


Fig. 1. Principal values of  $f'$  and  $f''$  tensors derived from absorption data (curves) and diffraction data (points) as described in the text. Solid lines and circles for  $\sigma$ , broken lines and open circles for  $\pi$ .

#### 4. Theory of phase determination

We quote some algebra of the MAD method as a basis for the theory of the new method. For the case that one type of atom exhibits significant anomalous scattering, Karle (1989) gives several forms of the equations that relate the structure-factor magnitude  $|F_{\lambda}|$  of reflection  $\mathbf{h}$  at wavelength  $\lambda$  to the magnitudes and phase differences of contributions of different sets of atoms. His equation (21), with some change of notation, is

$$|F_{\lambda}|^2 = \chi_5 + g_1\chi_2 + g_2\chi_6 + g_3\chi_7. \quad (3)$$

This equation is true for reflection  $-\mathbf{h}$  if the sign of  $g_3$  is changed. Functions which are independent of wavelength are

$$\chi_2 = |F_2^n|^2, \quad (4)$$

$$\chi_5 = |F_t^n|^2, \quad (5)$$

$$\chi_6 = |F_t^n||F_2^n| \cos \Delta, \quad (6)$$

$$\chi_7 = |F_t^n||F_2^n| \sin \Delta, \quad (7)$$

$$\Delta = \varphi_t^n - \varphi_2^n. \quad (8)$$

Here  $F_2^n$  is the structure factor for the set of atoms with anomalous scattering, but calculated without dispersion terms;  $F_t^n$  is similar but includes all atoms and  $\varphi$  signifies phase. Coefficients which change with wavelength (and in our case with azimuth) are:

$$g_1 = (f'/f^0)^2 + (f''/f^0)^2, \quad (9)$$

$$g_2 = 2f'/f^0, \quad (10)$$

$$g_3 = 2f''/f^0. \quad (11)$$

Observations of  $|F_{\lambda}|$  at four wavelengths, or Bijvoet pairs at two wavelengths, are sufficient to determine the four  $\chi$ 's by solution of linear equations, leading to a unique solution for the three independent unknowns  $|F_t^n|$ ,  $|F_2^n|$  and  $\Delta$ . With  $n$  different types of anomalous scatterers the equations are similar, but

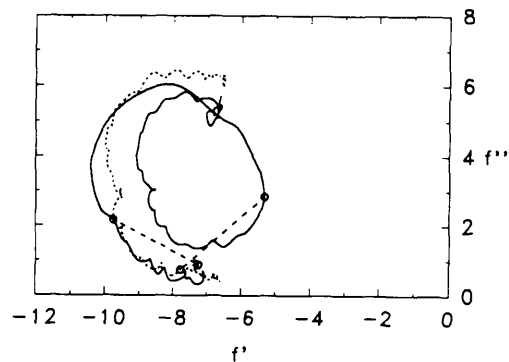


Fig. 2. Plots of  $f' + if''$  in the complex plane for  $\sigma$  (solid curve) and  $\pi$  (broken curve) polarizations. Tie lines connect points for the photon energies of Fig. 3.

there are  $2n+1$  independent unknowns and  $(n+1)^2$   $\chi$  functions.

Some of the complications of multiple-valued structure factors for the general case of tensor scattering are described elsewhere (Templeton & Templeton, 1982, 1988*b*; Fanchon & Hendrickson, 1990). Here we make some approximations which simplify the theory and its application. A more rigorous treatment, similar to that of Fanchon & Hendrickson (1990), is appropriate in the final stages of phase determination. The diffraction equations take a simpler form when (a) the radiation has complete linear polarization with electric vector perpendicular to the plane of scattering, (b) all anomalous atoms have tensors with the same magnitudes and orientation and (c) the  $sp'$  scattering factor can be neglected. Then  $f'$  and  $f''$  are single valued at each azimuth and (3) to (11) can be used without any change. The only difference from the MAD method is that azimuthal angle takes the place of wavelength. It makes sense to combine the two methods and change both wavelength and azimuth. It is shown below that this procedure can reverse some of the polarization effects and help separate them from experimental errors.

To test the phasing method with centrosymmetric vanadyl sulfate hydrate we neglected imaginary terms and assigned to each vanadium atom the same tensor with unique direction parallel with  $\mathbf{c}^*$ . Neither approximation introduces much error. Then the atomic scattering factor for vanadium is

$$f(\psi) = \mathbf{s}^T \mathbf{f} \mathbf{s} = f^0 + f'_\pi + \delta' \cos^2 \alpha, \quad (12)$$

where  $\psi$  is the azimuthal angle,  $\alpha$  is the angle between  $\mathbf{s}$  and  $\mathbf{c}^*$ , and  $\delta' = f'_\sigma - f'_\pi$ . For reflections with  $\mathbf{h} \perp \mathbf{c}^*$ ,  $\alpha$  changes at the same rate as  $\psi$  and the method works best. As  $\mathbf{h}$  approaches  $\mathbf{c}^*$  the range of  $\alpha$  is less, the modulation of  $f(\psi)$  diminishes and finally the method fails. With neglect of imaginary terms, one can write the total structure factor at wavelength  $\lambda$  and angle  $\psi$  as

$$F_{\lambda\psi} = F_i^n + F_2^n [f(\psi) - f^0] / f^0. \quad (13)$$

From (12) and (13) one gets

$$F_{\lambda\psi} = F_i^n + F_2^n (g_4 + g_5 \cos^2 \alpha), \quad (14)$$

$$g_4 = f'_\pi / f^0, \quad (15)$$

$$g_5 = \delta' / f^0. \quad (16)$$

In (14),  $F_{\lambda\psi}$  is a linear function of  $\cos^2 \alpha$  with slope  $g_5 F_2^n$  and intercept  $F_i^n + g_4 F_2^n$ . Let  $S$  and  $Y$  be the slope and intercept of a plot of  $|F_{\lambda\psi}|$  vs  $\cos^2 \alpha$ . Then the equations

$$F_2^n = S / g_5, \quad (17)$$

$$F_i^n = Y - S g_4 / g_5, \quad (18)$$

give  $F_2^n$  and  $F_i^n$  with signs consistent with positive  $F_{\lambda\psi}$  and thus their sign relation to each other is

determined. When  $S$  has the same sign as  $\delta'$ ,  $F_2^n$  has the same sign as  $F_{\lambda\psi}$ .

For noncentrosymmetric crystals the imaginary terms are necessary and (14) is not valid but another approximate formula may be useful. If the tensor is uniaxial, the atomic scattering factor (for  $ss$  scattering) is

$$f(\psi) = f^0 + f'_\pi + i f''_\pi + \delta \cos^2 \alpha, \quad (19)$$

$$\delta = f'_\sigma - f'_\pi + i(f''_\sigma - f''_\pi) = |\delta| \exp(i\varepsilon). \quad (20)$$

Here  $\varepsilon$  is the phase of  $\delta$  in the complex plane. The dispersion effects in  $F$  consist of terms proportional to  $f'_\pi$ ,  $f''_\pi$  and  $|\delta|$  with phases  $-\Delta$ ,  $\pi/2 - \Delta$  and  $\varepsilon - \Delta$  relative to  $F_i^n$ . If dispersion effects are small relative to the total structure factor, the projection of  $F_{\lambda\psi}$  on  $F_i^n$  is a good approximation of  $|F_{\lambda\psi}|$ :

$$|F_{\lambda\psi}| \approx |F_i^n| + |F_2^n| [g_4 \cos \Delta + g_6 \sin \Delta + g_7 \cos(\Delta - \varepsilon) \cos^2 \alpha], \quad (21)$$

$$g_6 = f''_\pi / f^0, \quad (22)$$

$$g_7 = |\delta| / f^0. \quad (23)$$

Again  $|F_{\lambda\psi}|$  is a linear function of  $\cos^2 \alpha$ , but now its slope is  $g_7 |F_2^n| \cos(\Delta - \varepsilon)$ . The sign of the slope limits  $\Delta$  to a semicircle and this slope is steepest when  $\Delta = \varepsilon$  or  $\Delta = \pi + \varepsilon$ . The corresponding slope for a Bijvoet mate is  $g_7 |F_2^n| \cos(\Delta + \varepsilon)$  and steepest slopes occur when  $\Delta = -\varepsilon$  or  $\Delta = \pi - \varepsilon$ . As the wavelength is changed through a polarized resonance, the real part of  $\delta$  changes sign and  $\varepsilon$  covers a wide range of angles. Thus a combination of observations of a Bijvoet pair at several wavelengths has diverse opportunities for phase indications regardless of the value of  $\Delta$ .

## 5. Experimental phase determination

Plots in Fig. 3 of  $|F_{\lambda\psi}|^2$  vs  $\psi$  for photon energies on either side of the absorption line are examples of strong anisotropy of scattering. These data have been corrected for absorption as described above. The tie lines shown in Fig. 2 show how  $f$  changes in the complex plane as the crystal is turned; the real component of the change is what is effective here. The reversal of the anisotropy when  $\lambda$  is changed is evidence that it arises from the sign change of  $\delta'$  rather than from an error in the absorption factor; the latter is nearly the same at both wavelengths. The plots of  $|F_{\lambda\psi}|$  vs  $\cos^2 \alpha$  (Fig. 4) are linear in agreement with (14). We attribute the scatter of the points mainly to instability in  $\lambda$  to which  $\delta'$  is very sensitive. For 420 the slopes of the two lines have the same signs as  $\delta'$ ; thus  $F_2^n$  has the same sign as  $F_{\lambda\psi}$  and (18) yields +31 and +36 for  $F_i^n$ . The value calculated from the known structure is +32. For 430, the reversal of slopes for the two photon energies shows that  $F_2^n$  and  $F_{\lambda\psi}$  have opposite signs. The second term in (18) is

larger than the first and  $F_1^n = -11$  and  $-6$  relative to positive  $F_{\lambda\psi}$  and negative  $F_2^n$ . The correct value is  $-10$ .

The effects of anisotropic absorption are comparable to those caused by  $\delta'$  and the absorption correction was essential for agreement with theory. Nevertheless, these phase results were evident when the raw data for the two wavelengths were compared.

One does not need so many data for this method to work. Two or three points at the right azimuths are enough. In the larger data sets with three azimuths per reflection, many correct relative signs could be recognized. The difference of slopes at the two wavelengths is a more reliable signal than is a single slope because of cancellation of some of the errors.

### 6. Discussion

The  $f'$  values measured by the two techniques are in good agreement except that less anisotropy is observed in the diffraction experiments, probably because of the larger  $\Delta E$  of the (111) monochromator. This anisotropy is sufficient to cause drastic effects

on diffraction intensities, yet it is not unusually large. Similar magnitudes of  $\delta'$  were found in  $\text{UO}_2^{2+}$  and two to three times larger ones in  $\text{BrO}_3^-$ ,  $\text{PtCl}_4^{2-}$  and Se bonded to C (Templeton & Templeton, 1982, 1985a, b, 1988b).

Rigorous correction for absorption remains an unsolved problem for dichroic crystals. The strategy that succeeded here, to use the absorption parameter for the largest component, is a first-order approximation which may be useful elsewhere.

That phase information is contained in the effects of polarized dispersion has already been demonstrated by experiments with forbidden reflections (Templeton & Templeton, 1987). The method described here is much more general. That the polarized-dispersion method can solve the phase problem with a single wavelength is shown here for a simple centrosymmetric case. In principle, with Bijvoet pairs, it can do the same for noncentrosymmetric crystals. It is more powerful if more than one wavelength is used and then it is an extension of the MAD method. In that mode it may give access to greater variety of values of  $f$  in the complex plane, may have some

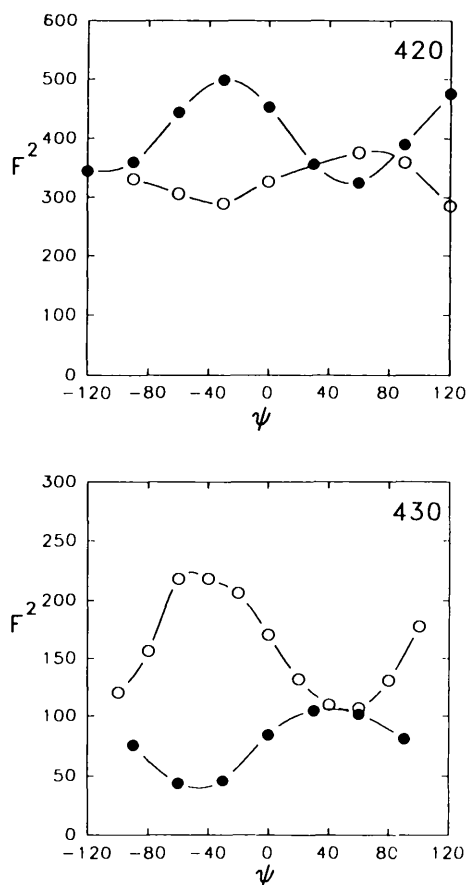


Fig. 3. Plots of  $|F|^2$  vs  $\psi$  for reflections 420 and 430 at 5467.7 eV (open circles) and 5470.5 eV (solid circles).

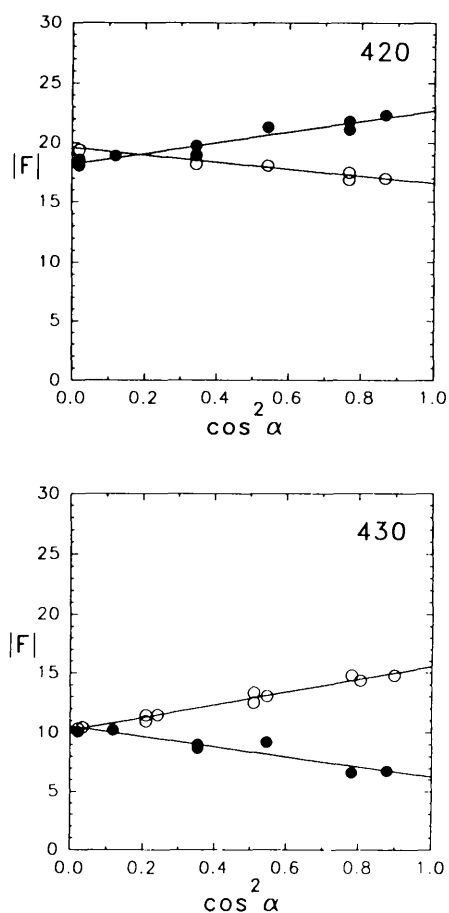


Fig. 4. Plots of  $|F|$  vs  $\cos^2 \alpha$  for data of Fig. 3.

advantages for design of experiments and may give some cancellation of experimental errors. Advantageous or not, the effects of anisotropy need attention when the MAD method is used with any crystal which exhibits X-ray dichroism.

To use the method one must somehow find the orientations of the atomic tensors. Absorption spectroscopy gives that tensor directly if there is only one orientation. Otherwise it gives a macroscopic tensor which is an average of atomic tensors. To find the atomic tensors then may be easy, difficult or impossible, depending on how many there are and what help is given by symmetry, by knowledge from other crystals, or from a partial solution of the structure in another way.

Here we have shown that polarized dispersion by itself can determine phases in simple cases. Perhaps more important is the implication that this phase information can enhance the power of the MAD method.

We thank the many staff members of SSRL whose assistance made this work possible. We are particularly indebted to Dr Michael Soltis. We thank Eric Fanchon and Wayne Hendrickson for a copy of their manuscript in advance of publication. This research was supported by the National Science Foundation under grants CHE-8515298 and CHE-8821318. It was done in part at SSRL which is supported by the Department of Energy, Office of Basic Energy Sciences; and the National Institutes of Health, Biotechnology Resource Program, Division of Research Resources. It used some facilities of the Lawrence Berkeley Laboratory, supported by the Director, Office of Energy Research, Office of Basic Energy Sciences, Chemical Sciences Division of the US Department of Energy under contract no. DE-AC03-76SF00098.

## APPENDIX

### Anisotropy matrix and macroscopic absorption tensor

The uniaxial atomic absorption tensor in a Cartesian system with  $z$  along the unique axis is

$$\boldsymbol{\mu}_i = \begin{pmatrix} \mu_\pi & 0 & 0 \\ 0 & \mu_\pi & 0 \\ 0 & 0 & \mu_\sigma \end{pmatrix}. \quad (24)$$

If expressed in terms of the average  $\mu_a = (2\mu_\pi + \mu_\sigma)/3$  and the anisotropy  $\delta_\mu = \mu_\sigma - \mu_\pi$  this becomes

$$\boldsymbol{\mu}_i = \mu_a \mathbf{I} + \delta_\mu \mathbf{M}_i, \quad (25)$$

where  $\mathbf{I}$  is the identity matrix and  $\mathbf{M}_i$  is the atomic anisotropy matrix

$$\mathbf{M}_i = \begin{pmatrix} -1/3 & 0 & 0 \\ 0 & -1/3 & 0 \\ 0 & 0 & 2/3 \end{pmatrix}. \quad (26)$$

The scalar  $\mu_i$  for polarization  $\mathbf{e}$  is

$$\mu_i = \mathbf{e}^T \boldsymbol{\mu}_i \mathbf{e} = \mu_a + \delta_\mu \mathbf{e}^T \mathbf{M}_i \mathbf{e}. \quad (27)$$

Let  $(u, v, w)$  be a unit vector defining the unique axis of  $\mathbf{M}_i$  in a second Cartesian system. It can be shown by the rules for rotation of vectors and tensors that  $\mathbf{M}_i$  in this system is

$$\mathbf{M}_i = \begin{pmatrix} u^2 - 1/3 & uv & uw \\ uv & v^2 - 1/3 & vw \\ uw & vw & w^2 - 1/3 \end{pmatrix}. \quad (28)$$

In monoclinic crystals for each atom with axis vector  $(u, v, w)$  there is a symmetry-related atom with vector  $(u, -v, w)$ . The average anisotropy matrix, which corresponds to the macroscopic absorption, is

$$\mathbf{M} = \begin{pmatrix} u^2 - 1/3 & 0 & uw \\ 0 & v^2 - 1/3 & 0 \\ uw & 0 & w^2 - 1/3 \end{pmatrix}. \quad (29)$$

In  $\text{VOSO}_4 \cdot 5\text{H}_2\text{O}$  the V-O(1) bond vector  $\mathbf{r}$  is (0.0872, -0.0210, 0.1303) in unit-cell coordinates. The transformation

$$\begin{pmatrix} u \\ v \\ w \end{pmatrix} = \frac{1}{|\mathbf{r}|} \begin{pmatrix} a & 0 & c \cos \beta \\ 0 & b & 0 \\ 0 & 0 & c \sin \beta \end{pmatrix} \begin{pmatrix} x \\ y \\ z \end{pmatrix} \quad (30)$$

gives  $(u, v, w) = (0.0054, -0.1288, 0.9917)$ . Substitution in (29) gives (2).

Another form of (28) is valid for biaxial tensors. The elements of  $\mathbf{M}_i$  are

$$m_{jk} = \sum_{n=1}^3 \varepsilon_n u_{nj} u_{nk} \quad (31)$$

if  $\mu_1, \mu_2, \mu_3$  are the principal values in monotonic order of magnitude,  $\mu_a$  is their average,  $(u_{n1}, u_{n2}, u_{n3})$  is the unit vector for the direction of  $\mu_n$ ,  $\delta_\mu = (\mu_3 - \mu_1)$  and  $\varepsilon_n = (\mu_n - \mu_a)/\delta_\mu$ . This definition is identical with (28) if  $\mu_1 = \mu_2$ .

## References

- BEARDEN, J. A. (1967). *Rev. Mod. Phys.* **39**, 78-124.  
 COLE, H., CHAMBERS, F. W. & WOOD, C. G. (1971). *J. Appl. Phys.* **32**, 1942-1945.  
 CORK, J. M. (1927). *Philos. Mag.* pp. 688-698.  
 CROMER, D. T. (1983). *J. Appl. Cryst.* **16**, 437.  
 CROMER, D. T. & LIBERMAN, D. (1970). *J. Chem. Phys.* **53**, 1891-1898.  
 DMITRIENKO, V. E. (1983). *Acta Cryst.* **A39**, 29-35.  
 FANCHON, E. & HENDRICKSON, W. A. (1990). *Acta Cryst.* **A46**, 809-820.  
 GUSS, J. M., MERRITT, E. A., PHIZACKERLEY, R. P., HEDMAN, B., MURATA, M., HODGSON, K. O. & FREEMAN, H. C. (1988). *Science*, **241**, 806-811.  
 HENDRICKSON, W. A., PÄHLER, A., SMITH, J. L., SATOW, Y., MERRITT, E. A. & PHIZACKERLEY, R. P. (1989). *Proc. Natl. Acad. Sci. USA*, **86**, 2190-2194.  
 KARLE, J. (1989). *Acta Cryst.* **A45**, 303-307.

- KRAUSE, M. O. & OLIVER, J. H. (1979). *J. Phys. Chem. Ref. Data*, **8**, 329-338.
- OKAYA, Y. & PEPINSKY, R. (1956). *Phys. Rev.* **103**, 1645-1657.
- PHILLIPS, J. C., CERINO, J. A. & HODGSON, K. O. (1979). *J. Appl. Cryst.* **12**, 592-600.
- RAMASESHAN, S., VENKATESHAN, K. & MANI, N. V. (1957). *Proc. Indian Acad. Sci.* **46A**, 95-111.
- TACHEZ, M., THÉOBALD, F., WATSON, K. J. & MERCIER, R. (1979). *Acta Cryst.* **B35**, 1545-1550.
- TEMPLETON, D. H. & TEMPLETON, L. K. (1980). *Acta Cryst.* **A36**, 237-241.
- TEMPLETON, D. H. & TEMPLETON, L. K. (1982). *Acta Cryst.* **A38**, 62-67.
- TEMPLETON, D. H. & TEMPLETON, L. K. (1985a). *Acta Cryst.* **A41**, 133-142.
- TEMPLETON, D. H. & TEMPLETON, L. K. (1985b). *Acta Cryst.* **A41**, 365-371.
- TEMPLETON, D. H. & TEMPLETON, L. K. (1987). *Acta Cryst.* **A43**, 573-574.
- TEMPLETON, D. H. & TEMPLETON, L. K. (1988a). *J. Appl. Cryst.* **21**, 151-153.
- TEMPLETON, L. K. & TEMPLETON, D. H. (1988b). *Acta Cryst.* **A44**, 1045-1051.

*Acta Cryst.* (1991). **A47**, 420-427

## The Electron Distribution in Diamond: a Comparison Between Experiment and Theory

BY MARK A. SPACKMAN

*Department of Chemistry, University of New England, Armidale, NSW 2351, Australia*

(Received 9 November 1990; accepted 28 January 1991)

### Abstract

Deformation and valence electron densities in diamond are derived *via* Fourier summation and pseudoatom multipole refinement of the recently reported structure factors derived from X-ray *Pendellösung* beats [Takama, Tsuchiya, Kobayashi & Sato (1990). *Acta Cryst.* **A46**, 514-517]. The results are significantly different from those reported previously and are generally in excellent agreement with theoretical calculations.

### Introduction

Because of its simple structure, high symmetry and low thermal motion, diamond occupies a unique position in the history of electron-density studies. The electron distribution in diamond was first examined by X-ray diffraction by Brill, Grimm, Hermann & Peters (1939) in an attempt to compare the covalent bonding in diamond with the ionic bonding in NaCl. The data set collected by those authors was subsequently analysed by Brill (1950, 1959, 1960) and Carpenter (1960). A more accurate, absolutely scaled, data set was later obtained from a powder sample by Göttlicher & Wölfel (1959; referred to as GW), and it is this data set which has since been analysed by many workers (Weiss, 1964, 1966; Dawson, 1967, 1975; Dawson & Sanger, 1967; Kurki-Suonio & Ruuskanen, 1971; McConnell & Sanger, 1970; Stewart, 1973a, c; Harel, Hecht & Hirshfeld, 1975; Price & Maslen, 1978) usually supplemented by the value of the 'forbidden' 222 reflection measured by

Renninger (1937, 1955) or Weiss & Middleton (1965; see Dawson, 1967).

In this work we take advantage of the recent measurement of nine low-order structure factors using the *Pendellösung* beat method (Takama, Tsuchiya, Kobayashi & Sato, 1990; referred to as TTKS). These data are significantly different from those reported by GW, and a preliminary electron-density analysis performed by TTKS suggests that the resulting electron distribution is also somewhat different from those obtained previously. The new data, in conjunction with an independently measured value for the 222 reflection, deserve a careful critical analysis in the manner we have previously performed on silicon (Spackman, 1986) and germanium (Brown & Spackman, 1990). In this way we hope to ascertain the degree of current accord (or otherwise) between experiment and theory for this important archetype of covalent bonding and, with reference to the similar studies on silicon and germanium, explore the nature of any trends which may be revealed as we descend this column of the Periodic Table.

We analyse the recent *Pendellösung* data of TTKS combined with a measurement of the 222 reflection, pursuing both Fourier methods and a rigid pseudoatom model (Stewart, 1973b, 1976). Where possible, standard deviations (e.s.d.'s) in the results are determined from the estimated errors in the experimental observations and the curvature of the least-squares-error surface at the minimum. The structure of the present paper parallels the earlier study on silicon. In the following section we discuss details of the data set chosen for the study, then describe